Apparatus for transient absorption spectroscopy based on water-window high-order harmonic attosecond light source*

DENG Yimin[1], ZHANG Yu[1], LU Peixiang[2], CAO Wei[1,*]

1. School of Physics, Huazhong University of Science and Technology, Wuhan 430074, China
2. Wuhan National Laboratory for Optoelectronics, Wuhan 430074, China

Abstract

Transient absorption spectroscopy using soft X-ray coherent light sources as ultrafast probes holds significant potential applications in chemistry, biology, and materials science. This article presents the design of a transient absorption apparatus based on tabletop soft X-ray light sources. A short-wavelength infrared (SWIR) laser pulse is generated to drive the production of soft X-ray high-order harmonic attosecond sources. This SWIR pulse is spectrally broadened and temporally compressed into a few-cycle pulse (400 μJ, 16.5 fs, 1530 nm) by a hollow-core fiber compressor. The few-cycle SWIR pulse then drives the generation of attosecond soft X-ray high-order harmonic radiation, with the maximum photon energy extending into the water window region (>300 eV). The spectral resolution of the soft X-ray spectrometer is determined to be 334 meV at 243 eV. The remaining 800 nm pump pulse from the OPA system is combined with the high-order harmonic soft X-ray probe by using a hole mirror, forming a Mach-Zehnder interferometer with a timing jitter less than 10 fs during the one-hour data acquisition. This setup demonstrates the feasibility of performing time-resolved soft X-ray spectroscopy in a compact experimental configuration. Preliminary studies of transient absorption near the argon L-edge and carbon K-edge are conducted, demonstrating that this system can be used as a powerful tool for element-specific, time-resolved, and transition-channel-resolved investigations of electron dynamics.

Keywords: high-order harmonics; soft X-ray; transient absorption; water window

PACS: 32.30.–r; 32.80.–t; 33.20.Xx; 42.65.Re

doi: 10.7498/aps.74.20250550

cstr: 32037.14.aps.74.20250550

* The paper is an English translated version of the original Chinese paper published in Acta Physica Sinica. Please cite the paper as: DENG Yimin, ZHANG Yu, LU Peixiang, CAO Wei，**Apparatus for transient absorption spectroscopy based on water-window high-order harmonic attosecond light sources** . *Acta Phys. Sin.*, 2025, 74(15): 153201. doi: 10.7498/aps.74.20250550

1. Introduction

Transient absorption spectroscopy is an advanced experimental method for studying ultrafast dynamic processes. The principle of transient absorption spectroscopy is to use a pump beam as the excitation source to trigger the ultrafast process, and then record the time evolution of the process with a probe beam. After the probe light passes through the sample, the change of its absorption spectrum can reveal the transient information of the ultrafast process. With the continuous development of laser technology, the time resolution of transient absorption spectroscopy continues to improve. Especially in recent years, the attosecond pulse generation and measurement technology based on high-order harmonics has matured significantly, leading to rapid development of transient absorption spectroscopy with attosecond time resolution.

In 2009, the Max Planck Institute in Germany, in collaboration with a research team at the University of California, Berkeley, first observed the periodic motion of valence electron wave packets in krypton ions on a time scale of several femtoseconds using attosecond transient absorption spectroscopy (ATAS) based on inner shell excitation[1]. Since then, several research teams have extended the technology to the field of solid materials and carried out extensive application research. For example, researchers have used this technique to detect the tunneling ionization dynamic process[2] in silicon crystals, observe the dynamic Franz-Keldysh effect[3] in polycrystalline diamond, reveal the light-induced ultrafast phase transition[4] of VO_2, and study the light-induced ultrafast coherent demagnetization process in ferromagnetic alloys[5].

At present, the spectra of attosecond probes commonly used in attosecond transient absorption spectroscopy are mainly distributed in the extreme ultraviolet (XUV) band of 10 - 70 nm, which are mainly used to study the valence electron dynamics in substances. If the wavelength of the attosecond probe is further extended to the soft X-ray "water window" band (2.3 - 4.4 nm), the traditional near-edge absorption spectroscopy can be endowed with the attosecond time-resolved ability to realize the element-resolved and structure-resolved ultrafast electron dynamics detection of organic biomolecules, magnetic materials, etc. This technology has great potential for applications in biology, chemistry, and materials science. However, due to the HHG generation mechanism, the HHG in the water window band requires a high-energy short-wavelength infrared laser, and the conversion efficiency is low. These technical limitations make the development of attosecond transient absorption spectroscopy in the water window band relatively slow.

Until 2017, Pertot et al.[6] first extended the transient absorption spectroscopy based on high-order harmonics to the water window band, and used ultrafast spectroscopy to study the diabatic process in the photochemical reaction of carbon-containing molecules. Transient absorption in the water window band is characterized by a wide bandwidth and

high photon energy, which allows scientists to study the inner shell structure of a variety of atoms and molecules in this band. After that, the ultrafast dynamics of gas[7–13], liquid[14,15], organic material[16,17] and other substances were studied by using the transient absorption of water window band. At the same time, scientists also used the transient absorption of water window band to carry out research on molecular structure[18], gas-phase chemical reaction[19], and molecular state[20] in the process of electronic relaxation. These studies have used high-energy (pulse energy > 10 mJ) femtosecond lasers coupled with high-power optical parameter amplifier (OPA) systems. Although important progress has been made, their high equipment cost, complex maintenance requirements, and large experimental space have challenged the popularization of this technology in conventional laser laboratories.

To solve this problem, we designed a compact transient absorption spectroscopy setup based on a water-window high-order harmonic attosecond source. A Ti: sapphire femtosecond laser with pulse energy less than 4.5 mJ is used as the main driving source, and optical parametric amplification and hollow-core fiber pulse compression technology are combined to generate few-cycle short-wavelength infrared pulses with central wavelength of 1530 nm, pulse energy of 400 μJ and pulse width of 16.5 fs. The few-cycle SWIR pulse can interact with high-pressure helium to produce a supercontinuum soft X-ray attosecond source with photon energy greater than 300 eV. Based on this light source, we have carried out transient absorption spectroscopy experiments on argon, carbon dioxide and other gases. This work provides a new idea for attosecond transient absorption spectroscopy with K-shell excitation in conventional laser laboratories.

2. Introduction of ATAS Device Based on Soft X-ray Attosecond Light Source

The transient absorption spectroscopy setup based on a water-window high-order harmonic attosecond source is shown in Fig. 1. The whole setup mainly consists of four parts: generation and diagnosis of few-cycle short-wavelength infrared (IR) laser, generation of water window high-order harmonic attosecond light source, dual-wavelength pump-probe optical path and soft X-ray spectrometer. In brief, the 1440 nm signal light output by an OPA is compressed into a few-cycle short-wavelengthlength infrared (SWIR) laser pulse by using a hollow-core fiber-based nonlinear compression technique, and the few-cycle laser pulse interacts with a high-pressure gas target to produce a water-windowed attosecond light source. The water window attosecond source and the residual 800 nm pump light of the OPA system are combined and synchronized, and then

jointly focused on the sample to be measured for dual-wavelength pump-probe experiments. The soft X-ray spectrum after passing through the sample was recorded by a home-made high-precision XUV spectrometer. By simplifying the optical path and reducing the optical components to shorten the optical path, our experimental device has the advantages of shorter[7,8,21] optical path, simple structure and compact optical path compared with similar devices. The use of two-color pump-probe optical path reduces the requirement of pulse energy and makes it easier to manipulate the polarization, energy and other parameters of the experimental pump light. The multi-stage differential vacuum design scheme is used in the HHG gas target chamber, and the high-pressure gas can be added to meet the phase-matching condition of the soft X-ray source. At the same time, the chirped mirror, window, reflector and other key optical components used in the experiment are purchased from domestic manufacturers, which reduces the cost of the experiment and the difficulty of maintenance of the device. The device is described in detail in the following sections.

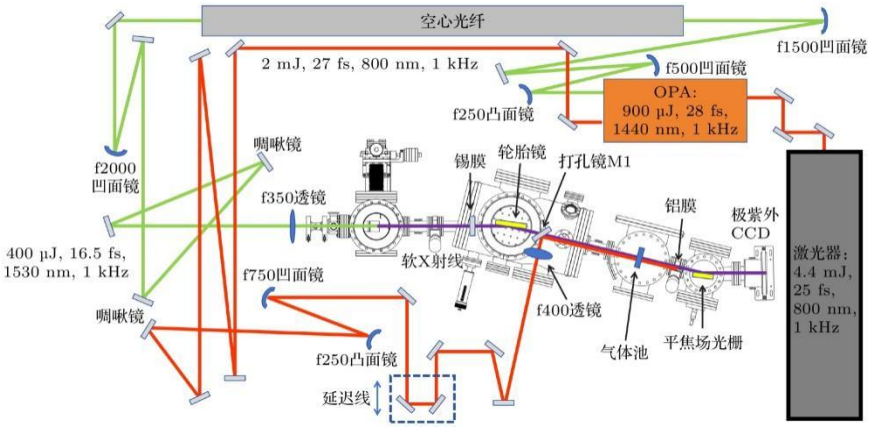

Figure 1. Schematic of transient absorption experimental carried by soft X-ray generated by few-cycle infrared laser.

2.1 Generation and diagnosis of few-cycle SWIR laser

A few-cycle short-wavelength infrared laser is required to drive a soft X-ray high-order harmonic attosecond source for soft X-ray spectral transient absorption experiments, and the nonlinear compression device is shown in Fig. 2. A 4.4 mJ, 25 fs, 800 nm, 1 kHz femtosecond laser from a Ti:sapphire femtosecond laser (Coherent Legend) was injected into a commercial OPA system (TOPAS-Prime) to obtain a 900 μJ, 28 fs, 1440 nm short-wavelength infrared laser. The expanded infrared laser is coupled into a hollow-core fiber with a length of 1 m and an inner diameter of 500 μm filled with 0. 5 bar argon (1 bar = 10^5 Pa) by a 1. 5 m concave mirror, and the infrared pulse spectrum is broadened by nonlinear effect (the infrared spectrum is shown in the Fig. 3), and a broadband spectrum

capable of generating few-cycle laser is obtained, wherein the central wavelength of the broadened spectrum is 1530 nm, and the spectral width is about 600 nm. The fiber system is encapsulated at both ends with a 1 mm thick window, a 1440 nm anti-reflection window at the input end and a 1 mm thick calcium fluoride window at the output end (to reduce the dispersion of the material). The output pulse energy of the hollow-core fiber is about 500 μJ, and the fiber coupling efficiency is about 62%. The broadened pulse is collimated by a concave mirror, and then the dispersion of the broadband pulse is compensated by a customized broadband chirped mirror (Shenzhen Haichuang Optics Co., Ltd., HR1170-1800 nm), and finally a 400 μJ few-cycle short-wavelength infrared pulse is obtained. The full width at half maximum (FWHM) of the compressed few-cycle short-wavelength infrared pulse is about 16.5 fs (as shown in the Fig. 4) measured by home built frequency resolved optical gating (FROG) system. The few-cycle infrared laser provides the necessary driving source for the subsequent generation of supercontinuum soft X-ray attosecond source.

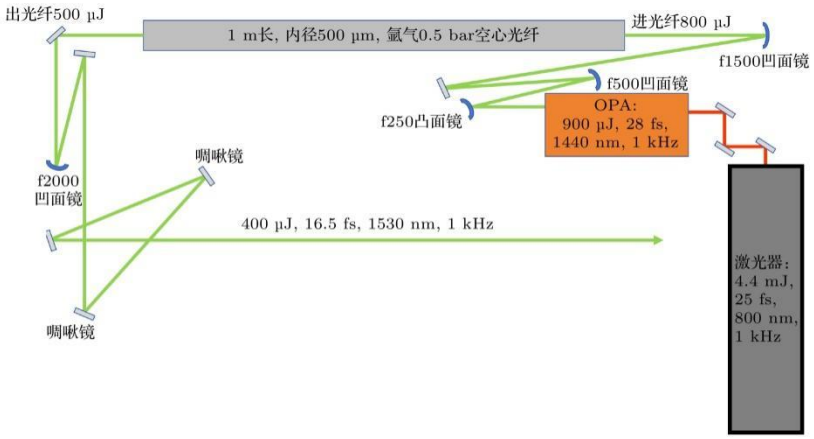

Figure 2. Schematic of few-cycle SWIR laser generation.

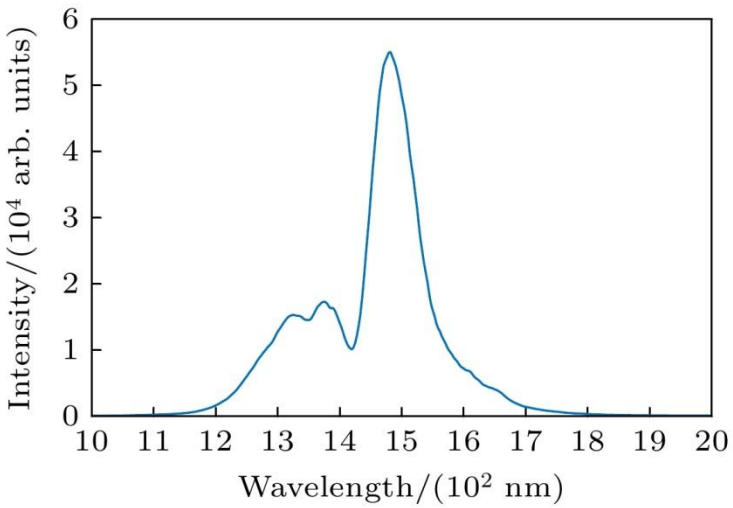

Figure 3. Spectrum of SWIR laser pulse after spectral broadening in hollow-core fiber.

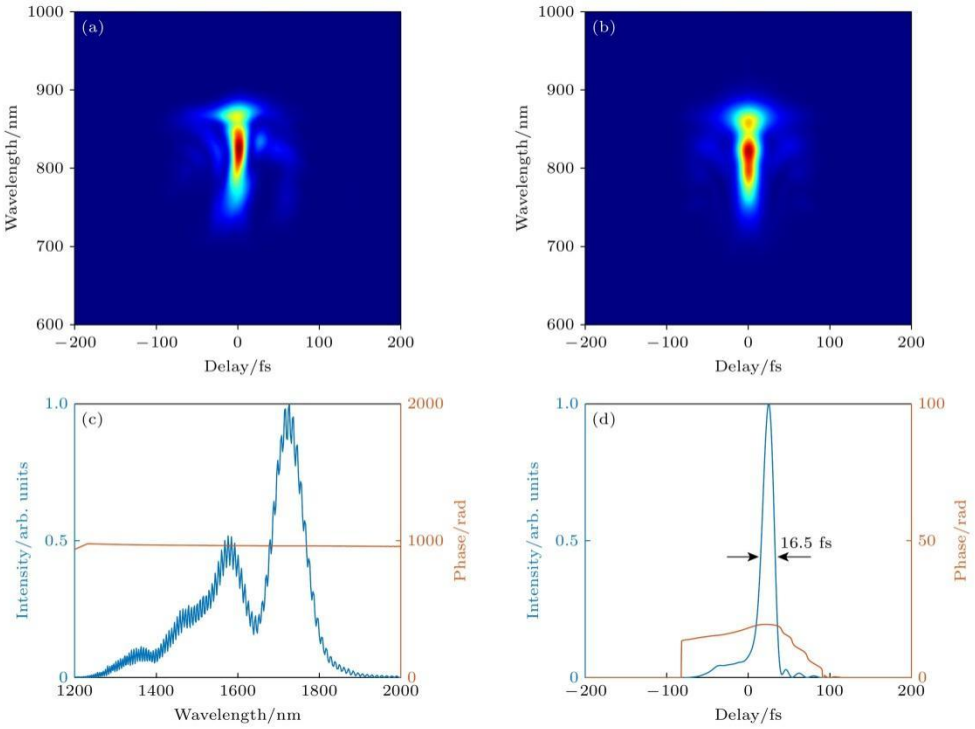

Figure 4. Results of FROG measurement: (a) Measured FROG trace; (b) reconstructed FROG trace; (c) reconstructed spectral amplitude and phase of the few-cycle SWIR laser pulse; (d) constructed temporal structure of the SWIR laser pulse.

2.2 Generation of high-order harmonic attosecond light source with water window

Soft X-ray high-order harmonics can be generated by directly focusing the compressed few-cycle short-wavelength infrared laser onto the gas target chamber with a lens with a focal length of 35 cm. In order to satisfy the phase-matching condition[22–24] for generating water window attosecond light source, the target chamber should be filled with rare gas at several atmospheres. Because the water window attosecond source will be rapidly absorbed when it propagates in non-vacuum conditions, it is necessary to design a differential vacuum system: the interaction region near the laser focus reaches a high pressure environment, and the pressure drops rapidly to the vacuum condition allowing the attosecond source to propagate after the attoseconds source is generated. The transmission optical elements (such as lens, window, etc.) Used in the experiment are made of calcium fluoride. Calcium fluoride can ensure more than 90% transmittance of the infrared laser band used in the experiment, while introducing less dispersion to minimize the time domain broadening of the few-cycle short-wavelength infrared laser.

The overall schematic diagram of the differential vacuum system is shown in Fig. 5. The dark blue chamber is the high harmonic generation target chamber. The gas used to generate soft X-ray high harmonics in the experiment is usually helium, and the pressure

optimized according to the high harmonic efficiency is about 3 bar; The orange chamber is sleeved outside the dark blue chamber, and the laser is focused to the rear end of the dark blue chamber to drill a small hole (about 100 μm in diameter), so that the two parts of the chambers are connected through the small hole to form a first-stage differential vacuum system, and the pressure of part of the orange chamber can be maintained at about 10 mbar by mechanical pumping; The yellow chamber outside the orange chamber is also connected with the orange chamber through a 1 mm small hole (the gray part in the Fig. 5) to form a second-stage differential vacuum system, and the pressure of the yellow chamber can be maintained at about 10^{-3} mbar by means of an on-chamber molecular pump to allow the water-window attosecond light source to propagate almost without attenuation. At the end of the differential vacuum system, a baffle with a 2 mm hole is placed, which not only helps to quickly adjust the propagation direction of the light path, but also blocks the rest of the infrared laser to a certain extent, so as to facilitate the subsequent transient absorption experiments.

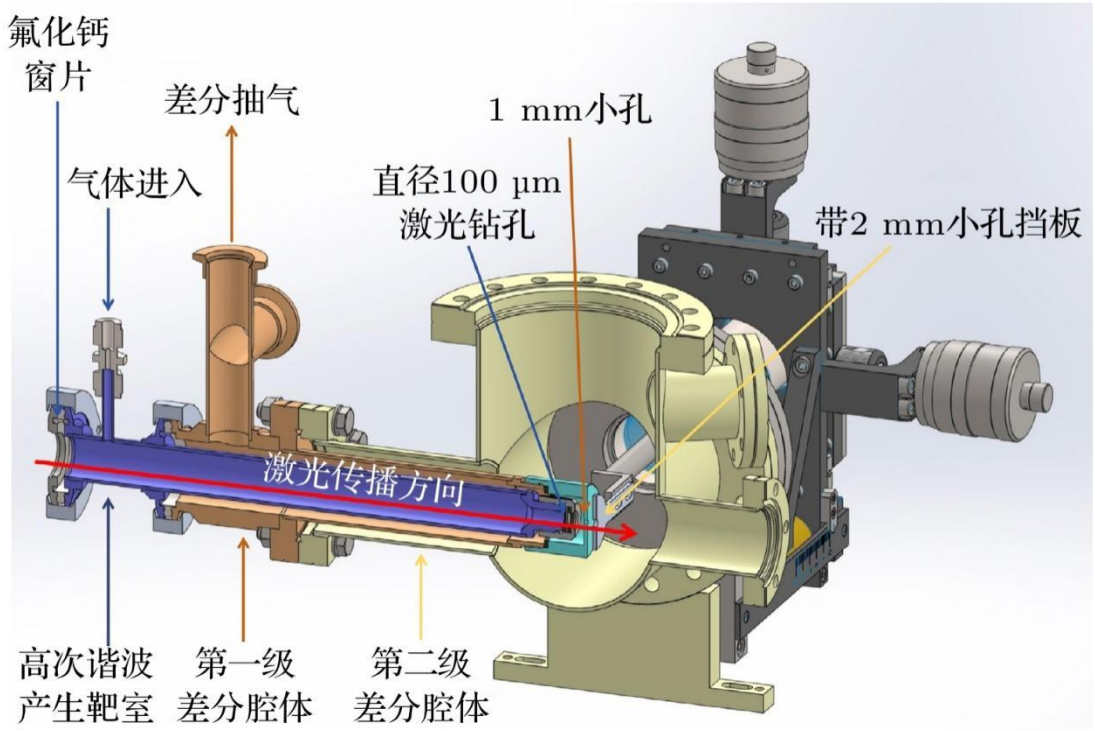

Figure 5. Cross section view of the gas target for soft X-ray high harmonic generation.

2.3 Soft X-ray spectrometer

A soft X-ray spectrometer was made to record and analyze the water window attosecond light source produced in the experiment. As shown in the Fig. 6, the generated soft X-ray high-order harmonic light source is incident on a flat-field grating (Shimadzu Optics, 30-006) with a reticle density of 1200 lines/mm through an adjustable slit, and the high-order harmonic spectrum after grating splitting is recorded by an X-ray CCD camera

(Princeton Instrument, PIXIO 400B), in which a 200 nm tin film and an aluminum film are placed in front of the slit to filter out the residual SWIR driving light, and the metal film can suppress the background and protect the camera.

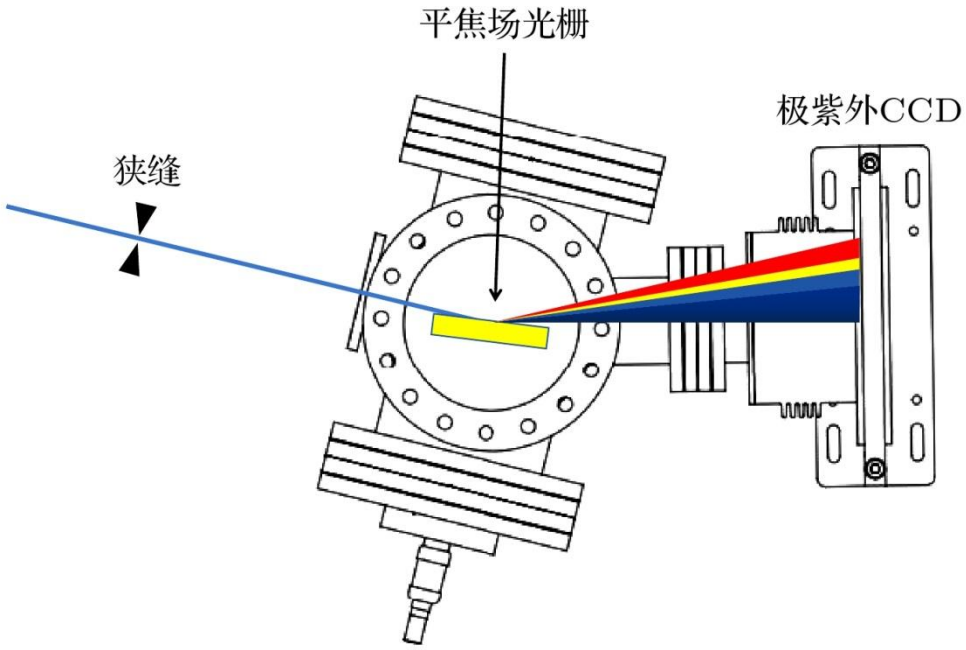

Figure 6. Home-built soft X-ray spectrometer.

The spectrometer can use the absorption lines of specific gases for energy calibration. The typical soft X-ray HHG spectra produced in the experiment are given by Fig. 7. It can be seen that the HHG produced by neon and helium are in the soft X-ray band. The highest energy of the harmonic generated by helium exceeds the carbon K-edge (284 eV) and reaches the water window band. The resolution and efficiency of the soft X-ray spectrometer can be improved by optimizing the grating position angle and the camera position. The acquisition of attosecond pulses mainly depends on the single-atom response (that is, the precise control of the time-domain waveform of the driving light), and the high-order harmonics in the soft X-ray band require a higher peak power of the driving light. The experimental phenomenon of soft X-ray continuum generation by few-cycle short-wavelength infrared driving generally indicates the generation of attosecond pulse train structure containing only a few attosecond pulses, which exhibits a supercontinuum structure due to the CEP instability of the driving light. The dispersion introduced by gas, metal film and other materials in the soft X-ray band is relatively small, so although the macroscopic propagation process will introduce a small amount of high-order dispersion bands to broaden the pulse width to a certain extent, the pulse width will usually be maintained at the attosecond scale. Therefore, the soft X-ray high-order harmonic light source generated in our experiment has the probe conditions for attosecond time-resolved spectroscopy. The Fig. 8 is the HHG spectrum of the absorption

target filled with argon, and the absorption lineshape near 243 eV corresponds to the L-shell excitation [9] of the argon $2p_{2/3}^{-1}4s$. The Gaussian response function was calculated by fitting the spatial integral of the absorption line shape in the[8] Fig. 8(b) with the convolution of the Lorentzian line shape of argon and the Gaussian function, and the resolution of the soft X-ray spectrometer was calculated to be about 334 meV.

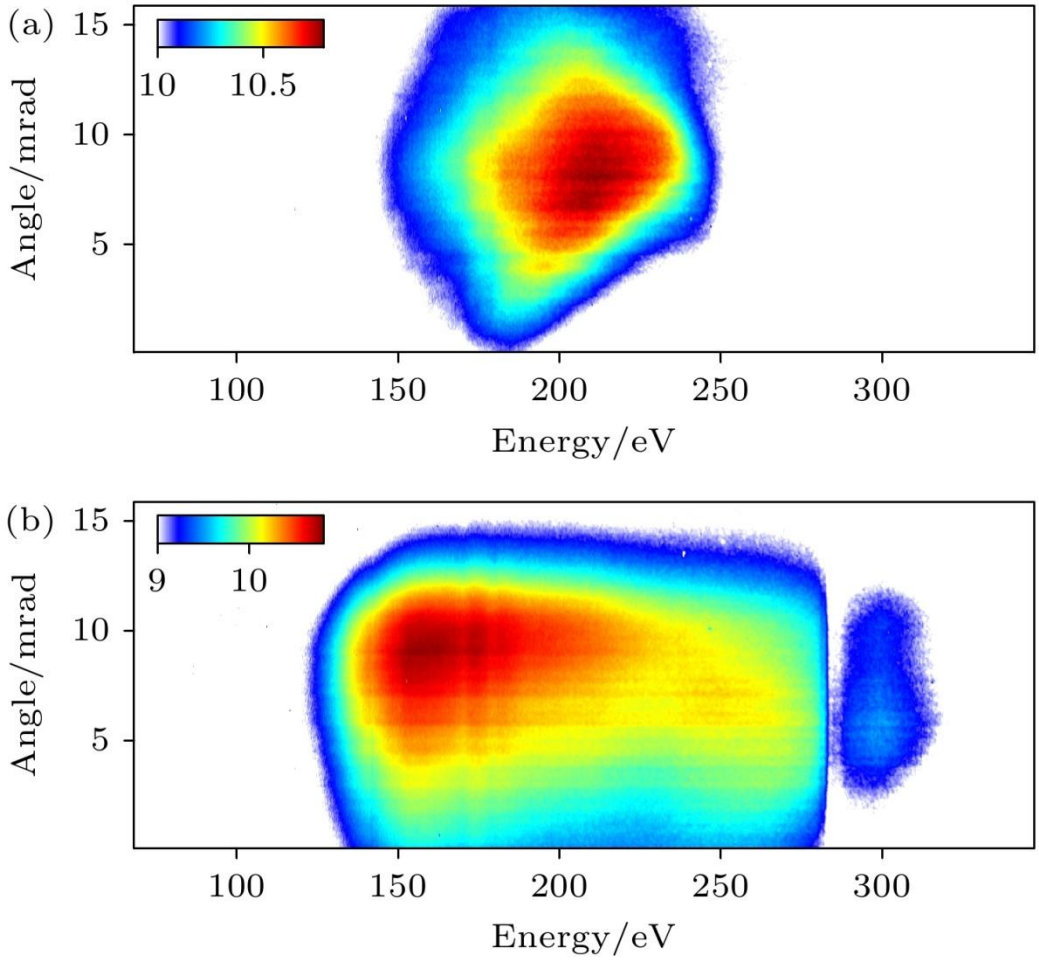

Figure 7. Soft X-ray high harmonic spectra from different gases: (a) Ne; (b) He.

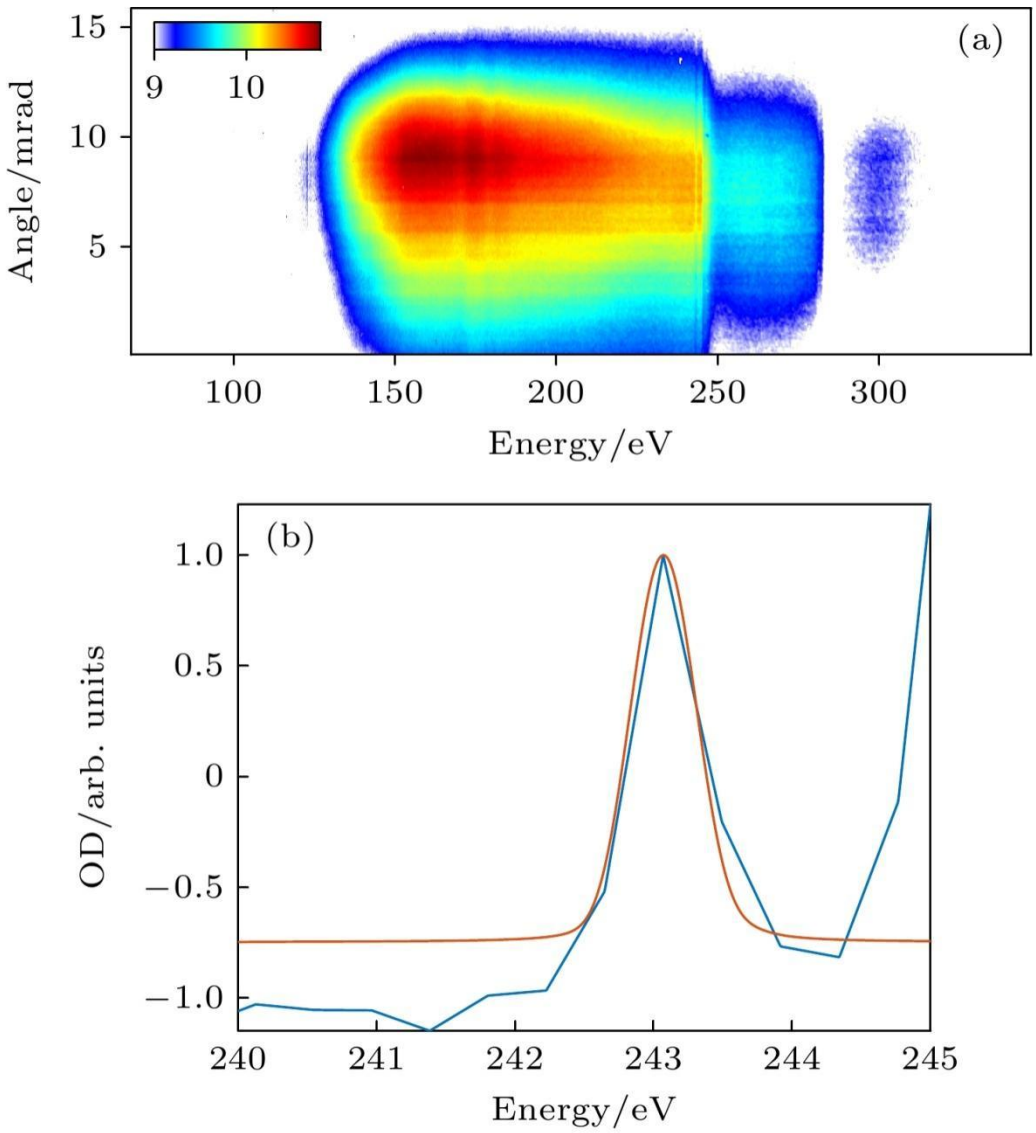

Figure 8. (a) Two-dimensional static absorption spectrum of Ar gas; (b) spatial integrated absorption spectrum in panel (a) near $2p_{2/3}^{-1}4s$ transition line of Ar (blue), red solid line represents the fitting by convoluting the Lorentz line shape with a Gaussian function, the fitting results indicate that the spectrometer resolution is approximately 334 meV.

2.4 Dual-wavelength pump-probe optical path

Based on the above light source, we set up a collinear pump-probe experimental optical path to track the ultrafast process. In the traditional Mach-Zehnder interferometer scheme, a high-energy laser pulse is split by a beam splitter to obtain the pump and probe light needed in the experiment. In this experiment, the energy of the signal light output by the OPA system is low, so the traditional beam splitting scheme based on single path light cannot be directly used. We use a dual-wavelength pump-probe experimental scheme at 1440 nm and 800 nm. As shown in the Fig. 1, the water window attosecond light source generated by the few-cycle infrared pulse is imaged onto the transient absorption gas

target through the toroidal mirror as the probe light. The remaining 2 mJ, 27 FS, 800 nm near-infrared laser of the OPA is used as the pump light to be guided into the vacuum chamber after passing through the delay line, and is focused by a lens with a focal length of 400 mm. The pump beam (NIR) and the probe beam (soft X-ray) are combined by a plane mirror with a 2 mm aperture. The aperture mirror allows the soft X-ray probe beam to pass through and reflects the external near-infrared pump beam. The focus of the combined beams is in the center of the transient absorption gas target. A movable mirror (M1 in the Fig. 1) is placed behind the hollow mirror, and when the mirror is moved into the optical path, the combined pump light and probe light can be reflected outside the vacuum chamber for spatiotemporal synchronous detection and optimization. For the dual-wavelength pump-probe scheme, the spatiotemporal synchronization of the two beams cannot be detected by the interference fringes. A 100 μm BBO nonlinear crystal with a cut angle of 20.5° is placed at the focus of the two reflected beams. When the two beams coincide in time and space, a sum frequency signal (about 500 nm green light) is generated in the BBO. According to the intensity of the sum frequency signal, the spatiotemporal synchronization of the pump and probe beams can be optimized.

The relative delay stability of the pump and probe light in the experiment is the key index affecting the resolution of the transient absorption experiment. The relative delay stability of the two beams is characterized by measuring the variation of the center wavelength of the combined signal with time[21]. The Fig. 9(a) is the change of the spectrum of the sum frequency signal measured by the spectrometer with the delay, and the place where the energy of the sum frequency signal is the strongest corresponds to zero delay. It can be seen that the spectrum of the sum signal is red-shifted with the increase of the delay. The variation of the center wavelength of the sum signal with the relative delay time of the pump and probe light is given Fig. 9(b). It can be seen that the change of the center wavelength of the sum signal with the delay is approximately a linear relationship, and the proportional coefficient of 5. 9 FS/nm is obtained by linear fitting of the curve. The time stability of the optical path difference between the two beams can be deduced by fixing the position of the displacement stage and recording the change of the central wavelength of the sum frequency signal with time.

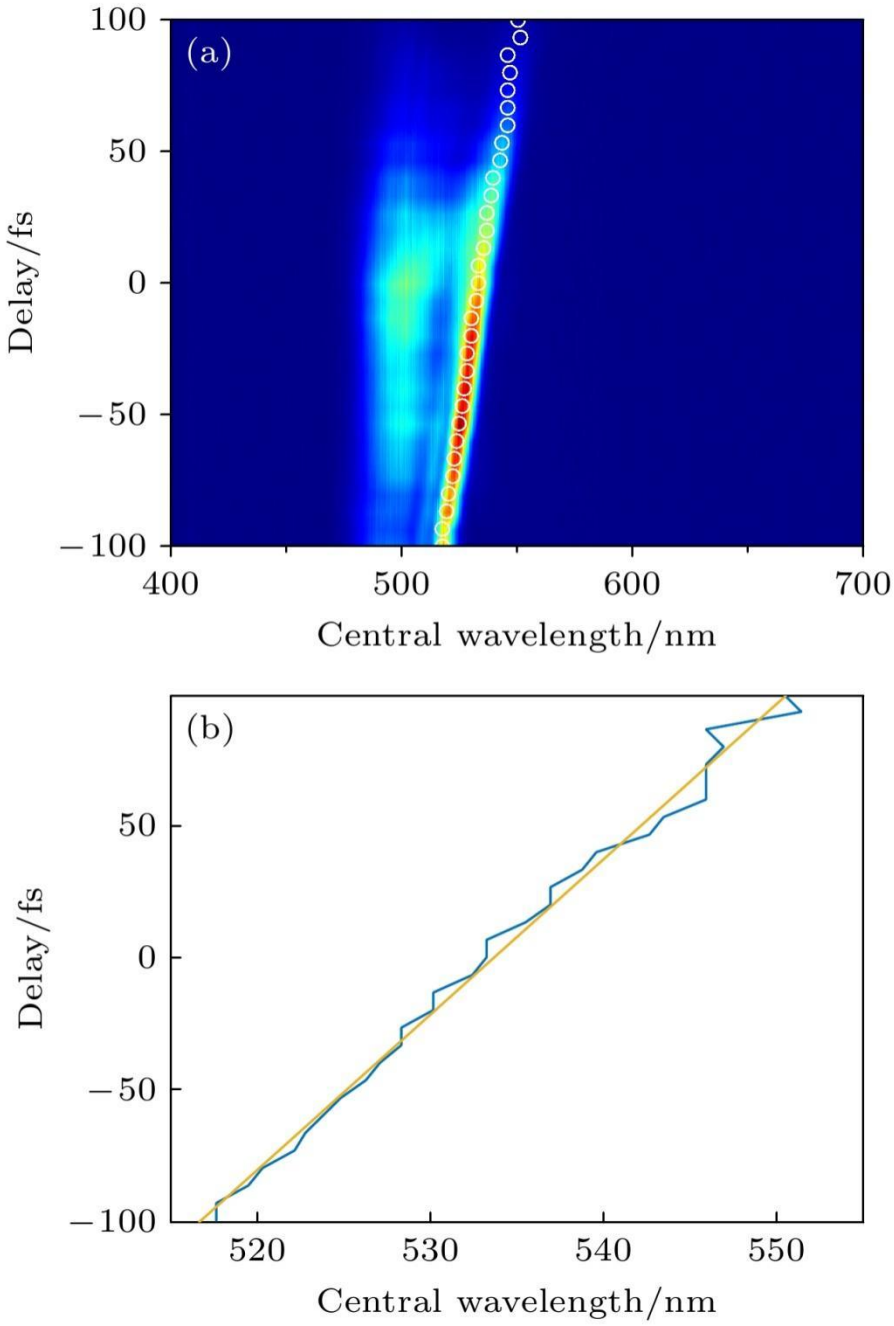

Figure 9. (a) Sum-frequency generation spectrum as a function of delay, the white circles indicate the positions of central wavelength; (b) central wavelength of the sum-frequency generation as a function of delay (blue), yellow line represents the linear fitting of the blue line.

The Fig. 10 is the test result of 3 hours, and it can be seen that the relative delay of the two lights increases monotonically with time. This is mainly due to the long optical path of the pump and probe light, and the change of temperature and beam pointing can cause the jitter of the relative delay. Usually, the acquisition time of a transient absorption experiment is about 1 h, and the relative delay of the two beams can be stabilized within 10 fs in this time range, which can meet the needs of most chemical reaction kinetics.

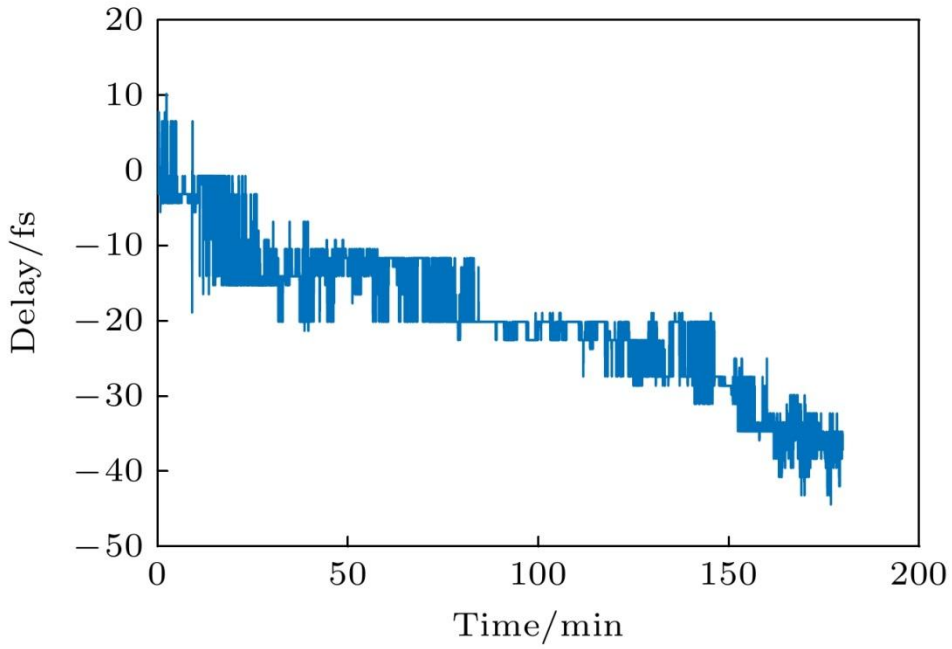

Figure 10. Relative delay drift over 3 h.

3. Experimental results of transient absorption spectroscopy for inner-shell excitation

3.1 Argon L-edge transient absorption spectrum

Transient absorption experiments were carried out using an attosecond source based on soft X-ray high harmonic generation. In the experiment, three spectra were collected at each delay point*τ*, and the integration time of each spectrum was 30 s. The final experimental data were obtained by averaging the three results. Optical density (OD) results are used for the absorption spectrum data obtained from the experiment, and OD is defined as $A(\tau) = -\log_{10}\frac{I(\tau)}{I_0(\tau)}$, where the reference spectrum I_0 is the spectrum without absorbing medium, and *I* is the spectrum after absorbing medium. Because HHG is a high-order nonlinear process, the weak fluctuation of the driving light power in the experiment will cause the jitter of the soft X-ray light power, so in principle, a reference spectrum should be collected at each delay point,, which reduces the experimental acquisition efficiency. In addition,, I_0 can also be reconstructed directly by low-pass filtering the *I* at each delay point. This method has been proved to be able to effectively eliminate the influence of the fluctuation of the soft X-ray source intensity on[25] during the experiment, which is also the scheme we adopted in the experiment. The Fig. 11 is the result of the transient absorption experiment of argon atoms, and the negative delay

indicates that the near-infrared laser arrives before the soft X-ray. For the interval far from zero delay (*τ*< - 40 FS or *τ*> 40 FS), the soft X-ray and near-infrared pulses are well separated in time, and the absorption edges of argon atoms L_1 – and $L_{2,3}$ can be clearly observed in the absorption spectrum. When the soft X-ray and near infrared pulses coincide, the absorption line positions of $2p_{3/2}^{-1}4s, 2p_{3/2}^{-1}5s/3d$ and $2p_{1/2}^{-1}5s/3d$ States are slightly blue-shifted due to the AC Stark effect, and the absorbance of these States decreases due to the dressing effect of near infrared light, which is consistent with the results reported by Barreau et al.[7]. The intensity of the absorption peaks of the $2p_{3/2}^{-1}4s, 2p_{3/2}^{-1}5s/3d$ and $2p_{1/2}^{-1}5s/3d$ and States as a function of the soft X-ray and near-infrared delays were extracted from the Fig. 11, respectively, and the results are shown in Fig. 12. Fitting the three curves in Fig. 12 with Gaussian function gives the time width within 20 fs, which also shows that the time resolution of our experiment is in the order of fs. In the next step, we hope to introduce the interferometer locking system to further improve the time stability of the delay displacement system to obtain higher time resolution and explore faster molecular dynamics processes.

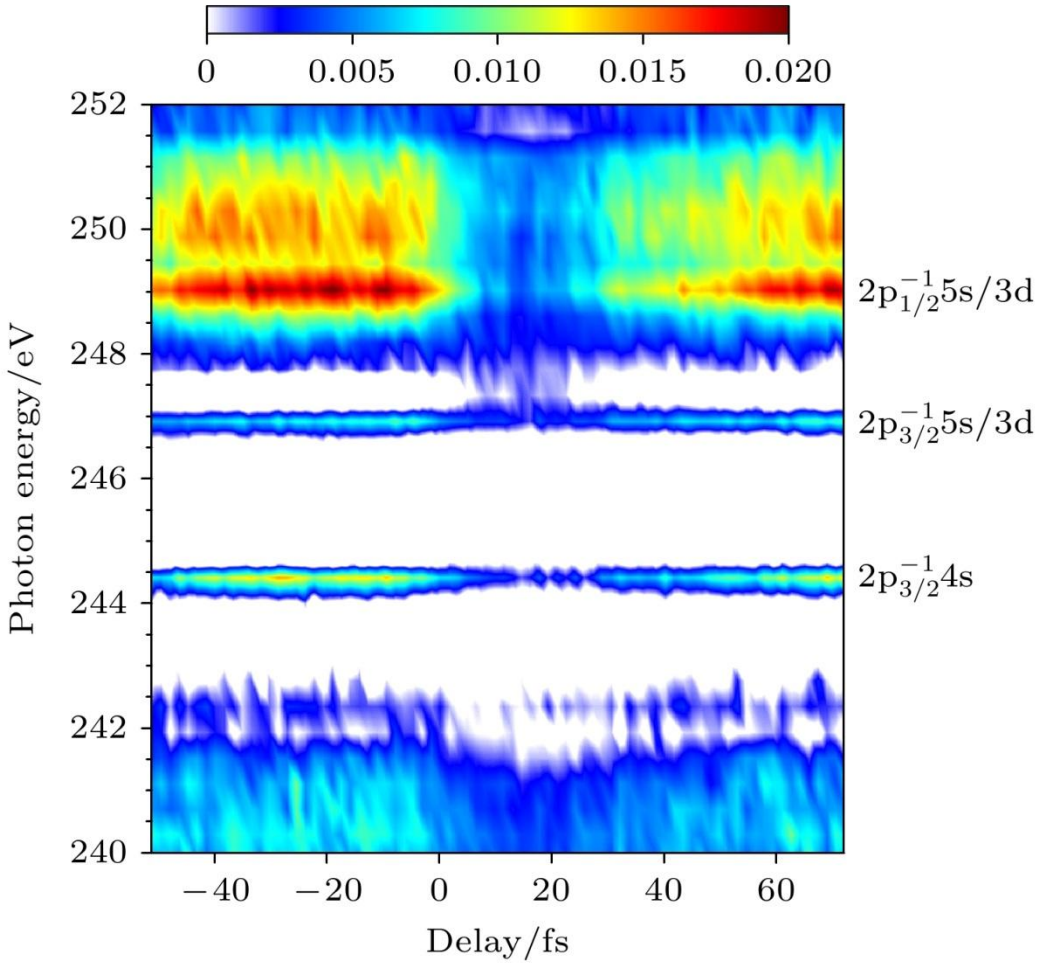

Figure 11. Experimental results of transient absorption of argon atoms.

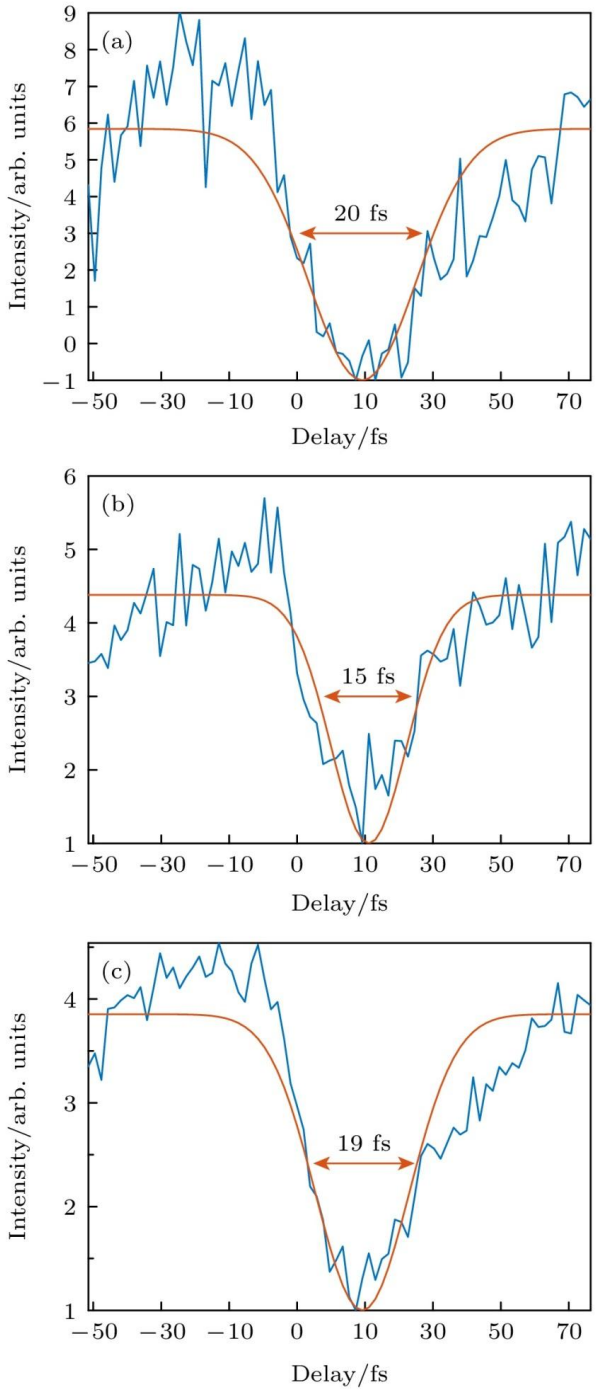

Figure 12. Intensity of the absorption peak $2p_{2/3}^{-1}4s$ **(a),** $2p_{2/3}^{-1}5s/3d$ (b) and $2p_{1/3}^{-1}5s/3d$ (c) as a function of delay. The solid blue lines are the measured results, and the red lines represent the Gaussian fitting.

3.2 CO_2 carbon K-edge transient absorption spectrum

The transient absorption spectrum of CO_2 molecule was studied by using the water window soft X-ray source with the maximum photon energy of more than 300 eV generated by high pressure helium as the probe light. The experimental results are shown

in the Fig. 13. Although the higher photon energy of HHG corresponds to a lower conversion efficiency, we can still identify three main characteristic absorption peaks near the carbon *K* edge in the experimental absorption spectrum. The three absorption peaks correspond to the excitation of 1s electron of carbon atom in CO_2 molecule: C 1s → π * (290 eV), C 1s → 3s (292 eV) and C 1s → 3p (294.5 eV), respectively.

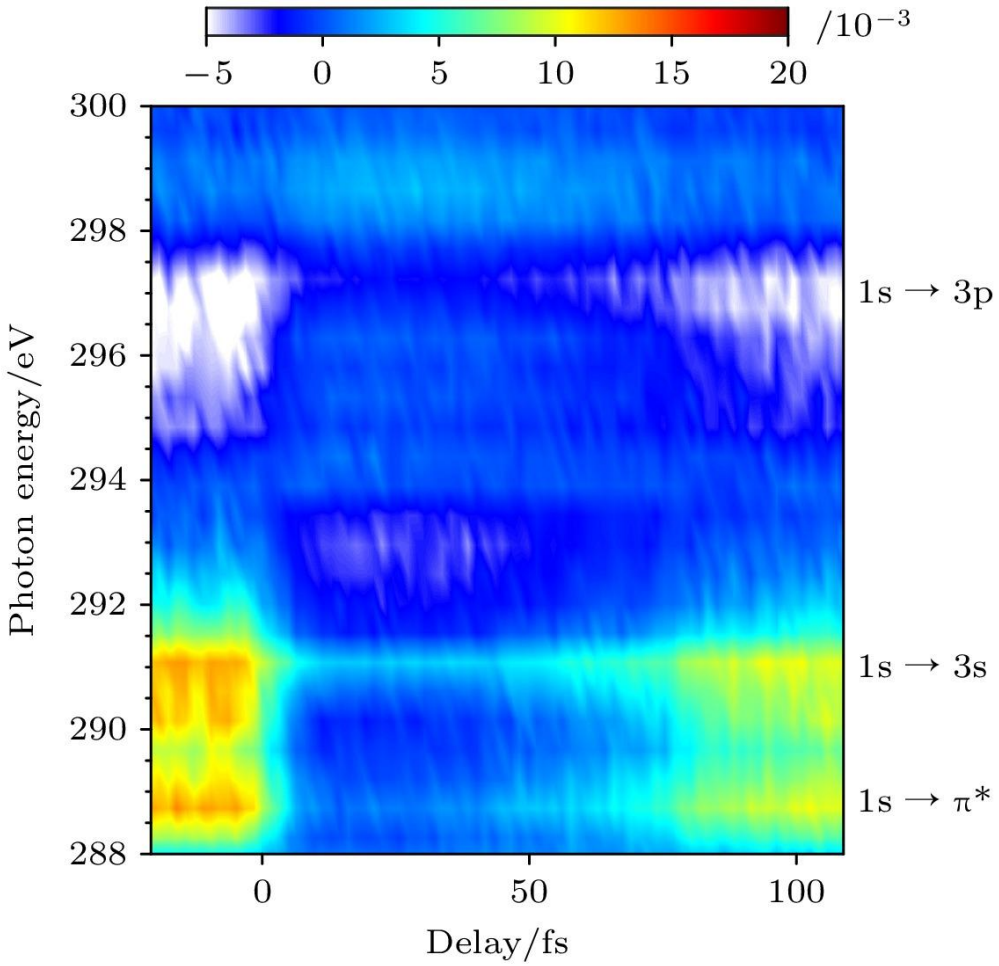

Figure 13. Experimental results of transient absorption of CO_2.

4. Conclusion

Using a femtosecond laser with moderate-pulse energy (< 4.5 mJ) as the driving source, we have designed and built a transient absorption spectroscopy setup based on a water-window high-order harmonic attosecond source. The device consists of a few-cycle short-wavelength infrared laser, a water window high-order harmonic attosecond light source, a dual-wavelength interferometer and a soft X-ray spectrometer. The whole set of device is compact in structure and simple in operation and maintenance. By combining optical parametric amplification and hollow-core fiber pulse compression, few-cycle

short-wavelength infrared pulses with a center wavelength of 1530 nm, a pulse energy of 400 μJ, and a pulse width of 16.5 fs are obtained. A soft X-ray high harmonic attosecond source with photon energy greater than 300 eV was produced by the interaction of the few-cycle pulse with a home-made high-pressure helium target. The time-space synchronization of the pump-probe optical path is realized by using a dual-wavelength experimental scheme, and the time stability is better than 10 fs within 1 h. The spectral resolution of the self-made X-ray spectrometer in the experiment is about 334 meV @ 243 eV. Transient absorption spectroscopy experiments of argon, carbon dioxide and other atomic and molecular gases have been carried out by using this device. The results show that the device can meet the dynamic research related to the excitation process of atomic and molecular inner shell electrons in energy resolution, time resolution and spectral range.

References

[1] Goulielmakis E, Loh Z H, Wirth A, Santra R, Rohringer N, Yakovlev V S, Zherebtsov S, Pfeifer T, Azzeer A M, Kling M F, Leone S R, Krausz F 2010 *Nature* **466** 739

[2] Schultze M, Ramasesha K, Pemmaraju C, Sato S, Whitmore D, Gandman A, Prell J S, Borja L J, Prendergast D, Yabana K, Neumark D M, Leone S R 2014 *Science* **346** 1348

[3] Lucchini M, Sato S A, Ludwig A, Herrmann J, Volkov M, Kasmi L, Shinohara Y, Yabana K, Gallmann L, Keller U 2016 *Science* **353** 916

[4] Lysenko S, Rua A, Vikhnin V, Jimenez J, Fernandez F, Liu H 2006 *Appl. Surf. Sci.* **252** 5512

[5] Zhang G P, Hübner W 2000 *Phys. Rev. Lett.* **85** 3025

[6] Pertot Y, Schmidt C, Matthews M, Chauvet A, Huppert M, Svoboda V, von Conta A, Tehlar A, Baykusheva D, Wolf J P, Wörner H J 2017 *Science* **355** 264

[7] Barreau L, Ross A D, Garg S, Kraus P M, Neumark D M, Leone S R 2020 *Sci. Rep.* **10** 5773

[8] Zinchenko K S, Ardana-Lamas F, Lanfaloni V U, Luu T T, Pertot Y, Huppert M, Wörner H J 2023 *Sci. Rep.* **13** 3059

[9] Chew A, Douguet N, Cariker C, Li J, Lindroth E, Ren X, Yin Y, Argenti L, Hill W T, Chang Z 2018 *Phys. Rev. A* **97** 031407

[10] Saito N, Sannohe H, Ishii N, Kanai T, Kosugi N, Wu Y, Chew A, Han S, Chang Z, Itatani J 2019 *Optica* **6** 1542

[11] Saito N, Douguet N, Sannohe H, Ishii N, Kanai T, Wu Y, Chew A, Han S, Schneider B I, Olsen J, Argenti L, Chang Z, Itatani J 2021 *Phys. Rev. Res.* **3**

043222

[12] Zinchenko K S, Ardana-Lamas F, Seidu I, Neville S P, van der Veen J, Lanfaloni V U, Schuurman M S, Wörner H J 2021 *Science* **371** 489

[13] Li J, Ren X, Yin Y, Zhao K, Chew A, Cheng Y, Cunningham E, Wang Y, Hu S, Wu Y, Chini M, Chang Z 2017 *Nat. Commun.* **8** 186

[14] Smith A D, Balčiūnas T, Chang Y P, Schmidt C, Zinchenko K, Nunes F B, Rossi E, Svoboda V, Yin Z, Wolf J P, Wörner H J 2020 *J. Phys. Chem. Lett.* **11** 1981

[15] Van Kuiken B E, Cho H, Hong K, Khalil M, Schoenlein R W, Kim T K, Huse N 2016 *J. Phys. Chem. Lett.* **7** 465

[16] Garratt D, Misiekis L, Wood D, Larsen E W, Matthews M, Alexander O, Ye P, Jarosch S, Ferchaud C, Strüber C, Johnson A S, Bakulin A A, Penfold T J, Marangos J P 2022 *Nat. Commun.* **13** 3414

[17] Sekikawa T, Saito N, Kurimoto Y, Ishii N, Mizuno T, Kanai T, Itatani J, Saita K, Taketsugu T 2023 *Phys. Chem. Chem. Phys.* **25** 8497

[18] Bhattacherjee A, Pemmaraju C D, Schnorr K, Attar A R, Leone S R 2017 *J. Am. Chem. Soc.* **139** 16576

[19] Bhattacherjee A, Leone S R 2018 *Acc. Chem. Res.* **51** 3203

[20] Scutelnic V, Tsuru S, Pápai M, Yang Z, Epshtein M, Xue T, Haugen E, Kobayashi Y, Krylov A I, Møller K B, Coriani S, Leone S R 2021 *Nat. Commun.* **12** 5003

[21] Lee J P, Avni T, Alexander O, Maimaris M, Ning H, Bakulin A A, Burden P G, Moutoulas E, Georgiadou D G, Brahms C, Travers J C, Marangos J P, Ferchaud C 2024 *Optica* **11** 1320

[22] Teichmann S M, Silva F, Cousin S L, Hemmer M, Biegert J 2016 *Nat. Commun.* **7** 11493

[23] Popmintchev T, Chen M C, Bahabad A, Gerrity M, Sidorenko P, Cohen O, Christov I P, Murnane M M, Kapteyn H C 2009 *Proc. Natl. Acad. Sci. U. S. A.* **106** 10516

[24] Pupeikis J, Chevreuil P A, Bigler N, Gallmann L, Phillips C R, Keller U 2020 *Optica* **7** 168

[25] Ott C, Kaldun A, Argenti L, Raith P, Meyer K, Laux M, Zhang Y, Blättermann A, Hagstotz S, Ding T, Heck R, Madroñero J, Martín F, Pfeifer T 2014 *Nature* **516** 374